

Massive thin accretion discs – I. Calculated spectra

Ari Laor and Hagai Netzer *School of Physics and Astronomy and The Wise Observatory,* Tel Aviv University, Tel Aviv 69978, Israel*

Accepted 1988 October 20. Received 1988 October 20; in original form 1987 July 14

Summary. We present detailed calculations of the structure and the spectrum of massive, geometrically thin, ‘bare’ accretion discs. The calculations are for an α -disc, with various assumptions about the viscosity and full relativistic corrections. The radiative transfer equations are solved using the Eddington approximation for an atmosphere with a vertical temperature gradient. All significant sources of opacity, for $T > 10^4$ K, are included, and all models are found to be optically thick throughout. The requirement of a geometrically thin disc forces a limit on the accretion rate, of $L < 0.3 L_{\text{edd}}$. Several previous disc calculations violate this limit and their results are questionable. All discs considered in this work are found to be radiation pressure dominated throughout the region where self-gravity dominates. Spectral changes due to electron scattering (modified blackbody and comptonization) are not significant in most models. The surface temperature is close to the effective temperature, even for regions where electron scattering effects are significant, due to the vertical temperature gradient, in contradiction to earlier findings. The upper limit on the accretion rate indicates that thin discs, with no corona, may not have enough soft X-rays to explain the observations of bright quasars. Relativistic effects modify the spectrum, considerably, at large viewing angles. We show several examples for this and calculate the angular dependence of the ionizing radiation and photons flux. This may have important implications on the modelling of AGN emission lines.

1 Introduction

A likely mechanism for powering Active Galactic Nuclei (AGN), is the release of gravitational energy by accretion on to a massive compact object (see review and references in Rees 1984 and Begelman 1985). A possible configuration is that of a geometrically thin accretion disc around a central black hole (BH).

The theory of accretion discs is described in Shakura & Sunyaev (1973, hereafter SS73) and Novikov & Thorne (1973, hereafter NT73), and is reviewed by Pringle (1981). Throughout this paper we refer to it as ‘the standard disc theory’. Stellar accretion discs, i.e. those around a solar mass white dwarf, neutron star or BH, have been studied extensively. Theoretical spectra for such systems have been computed by means of adding stellar atmospheres (Herter *et al.*

*Of the Raymond and Beverly Sackler Faculty of Exact Sciences.

1979; Wade 1984), or by calculating specific models for the disc atmosphere (Williams, King & Brooker 1987; Kriz & Hybeny 1987). Less attention has been paid to massive discs, i.e. those around massive BH. Some models have been calculated by Callahan (1977) and Sakimoto & Coroniti (1981), and a time-dependent structure was investigated by Lin & Shields (1986).

Shields (1978), Malkan & Sargent (1982) and Malkan (1983) suggested that the blue-ultraviolet continuum in quasars and other AGN is due to thermal emission from the surface of an accretion disc. Verification of this idea depends on accurate calculations of the disc spectrum that were not available at the time. Currently there are some simplified calculations, based on the local blackbody approximation (Malkan 1983; Bechtold *et al.* 1987; Wandel 1987), or the combination of stellar spectra (Kolykhalov & Sunyaev 1984; Sun & Malkan 1987). The most detailed calculation known to us is by Czerny & Elvis (1987) who include the effects of electron scattering.

In this paper we present new calculations for thin discs around massive BH. We use the Eddington approximation and a full treatment of electron and bound-free opacities to calculate the local spectrum. We integrate over the disc surface to obtain the observed spectrum at different viewing angles, taking into account all relativistic corrections. We assume a 'bare disc' – i.e. no corona or other scattering material above the disc. The calculations cover a large range in luminosity and demonstrate, in detail, the spectral dependence on the mass of the central source, the accretion rate and other parameters.

The plan of the paper is as follows: in Section 2 we introduce the basic equations and the standard solution, and calculate the local and the observed spectrum. We also discuss the requirements for a self-consistent model, and compare stellar and massive discs. In Section 3 we present disc spectra for a large range of parameters, and in Section 4 we discuss the implications of our results. A detailed comparison with the observed spectrum of AGN is deferred to another paper.

2 Calculations

2.1 BASIC EQUATIONS

The disc structure equations are taken from NT73 and Page & Thorne (1974, hereafter PT74), and include general relativistic treatment of non-rotating and rotating BH. In the following equations M is the mass of the central BH, R is the radial distance, R_{ms} is the radius of marginal stability (the inner radius of the disc), \dot{M} is the accretion rate, F_0 is the surface flux, Σ_0 is the surface mass density, V_r is the radial drift velocity of matter and W is the vertically integrated shear stress. The equations for the radial structure are:

angular momentum conservation:

$$W = \dot{M}/2\pi \sqrt{\frac{GM}{R^3} \frac{QC^{1/2}}{BD}}; \quad (1)$$

energy conservation:

$$F_0 = \frac{3GM\dot{M}}{8\pi R^3} \frac{Q}{BC^{1/2}}; \quad (2)$$

and rest mass conservation:

$$\dot{M} = 2\pi R \Sigma_0 V_r D^{1/2}. \quad (3)$$

Here A , B , C , D , E and Q are the general relativistic correction factors defined in NT73 and PT74, all approaching 1 at $R \gg R_{\text{ms}}$. For example, in equation (2) the correction factor $Q/BC^{1/2}$ replaces the Newtonian factor $1 - (R/R_{\text{ms}})^{-1/2}$ (see SS73). As a result the Newtonian efficiency for a non-rotating BH is 0.0825 while the true efficiency is 0.0572.

The vertical (z -coordinate) structure equations are:

the pressure balance:

$$\frac{dP}{dz} = \frac{\rho GMz}{R^3} \frac{B^2 DE}{A^2 C}; \quad (4)$$

the energy generation:

$$\frac{dq}{dz} = \frac{3}{2} \sqrt{\frac{GM}{R^3}} t_{r\phi} \frac{D}{C}; \quad (5)$$

and the radiative energy transfer:

$$q(z) = -\frac{c}{3\kappa\rho} \frac{du}{dz}. \quad (6)$$

Here P is the pressure, $t_{r\phi}$ the viscous stress, q the vertical radiation flux, u the radiation energy density, κ the opacity (in equation 6 κ is the Rosseland mean) and ρ the mass density.

In the present paper the radiative transfer is solved by means of the Eddington approximation for a grey atmosphere. This is valid when electron scattering dominates the opacity. We neglect convective energy transport which, according to Shakura, Sunyaev & Zilitinkevich (1978), amounts to less than half the total energy transport in the radiation pressure dominated part of the disc. For the viscous stress, $t_{r\phi}$, we use the conventional α -disc model assumption: $t_{r\phi} = \alpha P$. We consider three possible cases; (a) $P = P_r + P_g$, (b) $P = P_g$, and (c) $P = \sqrt{P_g P_r}$, where P_g is the gas pressure and P_r the radiation pressure. The first of these is probably thermally unstable in the inner, radiation pressure dominated part (SS76; Piran 1978). Cases (b) and (c) have been proposed for the case of turbulences generated by magnetic fields (Sakimoto & Coroniti 1981; Burm 1985; Lin & Shields 1986). In such cases energy production by dissipative processes may not be distributed throughout the disc, and could be concentrated, for example, in a thin corona. This may be inconsistent with the standard α -disc model.

Throughout this paper we assume $P_r > P_g$ and that electron scattering opacity [$\kappa(\text{es})$] dominates true absorption [$\kappa(\text{ab})$] everywhere (the so-called region a in SS73). These assumptions are discussed below and in Sections 2.2.2, 2.3.2 and 2.4.1. In all calculations we assume the following chemical composition: $X = 0.75$, $Y = 0.25$ and $Z = 0$.

In the solution for the vertical density profile we use the simplifying assumption that energy generation by viscosity is proportional to the density (SS73 and NT73, a more accurate relation, within the α -disc model, is given in equation 5). This gives:

$$q(z) = 2F_0 \Sigma(z) / \Sigma_0, \quad (7)$$

where

$$\Sigma(z) = \int_0^z \rho(z) dz$$

using equation (4) with $P = P_r$, equations (6) and (7) we get:

$$\Sigma(z) = GMc \frac{\Sigma_0}{2F_0 R^3 \kappa} z. \quad (8)$$

The assumption of a constant opacity inside the disc, $\kappa = \kappa(\text{es})$, makes the density independent of z . Alternatively, if energy transfer by convection is included, we get the density profile as calculated by Bisnovatyi-Kogon & Blinikov (1977) and Shakura *et al.* (1978).

The base of the photosphere (z_0) is found by equating the pressure exerted by the outgoing radiation to the local gravity:

$$\int \frac{F_\nu \kappa_\nu}{c} dv = \frac{GMz_0}{R^3} c_r. \quad (9)$$

For $\kappa(\text{ab}) \ll \kappa(\text{es})$, we get:

$$z_0 = \frac{F_0 \kappa(\text{es}) R^3}{cGM} c_r. \quad (10)$$

Where $F_0 = \int F_\nu dv$ and $c_r = B^2 DEA^{-2} C^{-1}$ (see equation 4). The above expression can also be deduced directly from equation (8). An approximate expression for z_0 , for the case $\kappa(\text{ab}) > \kappa(\text{es})$, is given in Section 2.3.2.

The standard solution for the thin α -disc (SS73; NT73) is given in terms of the dimensionless parameters:

$$m_9 = \frac{M}{10^9 M_\odot} \quad r = \frac{R}{R_g} \quad \text{and} \quad \dot{m} = \frac{\dot{M}}{38.8 m_9 M_\odot \text{ yr}^{-1}},$$

where $R_g = GM/c^2 = 1.47610^{14} m_9$ cm. The Eddington luminosity for pure hydrogen, $L_{\text{edd}} = 1.25 \times 10^{47} m_9$ erg s⁻¹, is related to \dot{M}_{edd} by $L_{\text{edd}} = \eta \dot{M}_{\text{edd}} c^2$, or $\dot{M}_{\text{edd}} = 2.22 m_9 / \eta M_\odot \text{ yr}^{-1}$, where η is the efficiency. We consider only two cases: a non-rotating and a maximally rotating BH (see Thorne 1974). We also neglect radiation absorption by the BH (see Cunningham 1976). For a non-rotating BH $\eta = 0.0572$ and thus $\dot{M}_{\text{edd}} = 38.8 m_9 M_\odot \text{ yr}^{-1}$, and for a maximally rotating one $\eta = 0.324$ and $\dot{M}_{\text{edd}} = 6.85 m_9 M_\odot \text{ yr}^{-1}$. With the above definitions $L = \dot{m} L_{\text{edd}}$ for a non-rotating BH and $L = 5.66 \dot{m} L_{\text{edd}}$ for a maximally rotating one.*

The standard solution for the local energy flux is:

$$F_0(r) = 1.2 \times 10^{19} \dot{m} m_9^{-1} r^{-3} c_1 \text{ erg s}^{-1} \text{ cm}^{-2} \quad (11)$$

and for the disc half-thickness:

$$z_0(r) = 3.9 \times 10^{15} \dot{m} m_9 c_2(r) \text{ cm}, \quad (12)$$

$c_1 - c_8$ are general relativistic correction factors that are functions of the parameters $A - Q$ introduced earlier. $c_1 - c_4$ are defined in NT73 (equation 5.9.10) and $c_5 - c_8$ are given by:

$$c_5 = B^{12/5} E D^{1/5} A^{-2} Q^{-2/5},$$

$$c_6 = Q^{2/5} B^{-2/5} D^{-1/5},$$

$$c_7 = B^4 D E^{13/9} Q^{-10/9} A^{-26/9},$$

$$c_8 = E^{-1/9} Q^{-2/9} A^{-2/9}.$$

*The above definitions of r and m are different from those given by SS73. This results in different coefficients in equations (11), (12), (13a) and (14a) compared with their equations (2.8)-(2.11).

All these factors approach unity for $r \gg 1$. The local nucleon number density, $N(r)$, and the local temperature at the centre of the disc, $T_c(r)$, depend on the viscosity law. Referring to the three possibilities introduced earlier we find that in case (a) [$t_{r\phi} = \alpha(P_r + P_g)$]

$$N(r) = 2.4 \times 10^7 \alpha^{-1} \dot{m}^{-2} m_9^{-1} r^{1.5} c_3 \text{ cm}^{-3} \quad (13a)$$

$$T_c(r) = 2.8 \times 10^5 m_9^{-1/4} \alpha^{-1/4} r^{-3/8} c_4 \text{ K}; \quad (14a)$$

in case (b) ($t_{r\phi} = \alpha P_g$)

$$N(r) = 2.9 \times 10^{15} \alpha^{-0.8} m_9^{-0.8} \dot{m}^{-0.4} r^{-0.6} c_5 \text{ cm}^{-3} \quad (13b)$$

$$T_c(r) = 2.9 \times 10^7 \dot{m}^{0.4} m_9^{-0.2} \alpha^{-0.2} r^{-0.9} c_6 \text{ K}; \quad (14b)$$

and in case (c) ($t_{r\phi} = \alpha \sqrt{P_g P_r}$)

$$N(r) = 7.3 \times 10^{11} m_9^{-0.88} \alpha^{-0.88} \dot{m}^{-1.11} r^{0.33} c_7 \text{ cm}^{-3} \quad (13c)$$

$$T_c(r) = 3.7 \times 10^6 m_9^{-0.22} \alpha^{-0.22} \dot{m}^{0.22} r^{-0.66} c_8 \text{ K}. \quad (14c)$$

Note that the density in the inner part of the disc is about two to three orders of magnitude greater in case (b) compared with case (a) and the central temperature is about one order of magnitude greater. The values of $N(r)$ and $T_c(r)$ in case (c) are intermediate between those two cases.

2.2 A COMPARISON OF MASSIVE AND STELLAR DISCS

There are many detailed calculations for stellar discs (e.g. Meyer & Meyer-Hofmeister 1982; Cannizzo & Wheeler 1984). Below we describe some of the important differences distinguishing a 'light' ($\sim 1 M_\odot$ central BH) for a 'massive' ($10^9 M_\odot$ central BH) disc.

2.2.1 Radiation versus gas pressure*

The ratio of radiation to gas pressure, for a completely ionized gas and $r \gg r_{\text{ms}}$, is:

$$P_r/P_g = 7.3 \times 10^9 m_9^{1/4} \dot{m}^2 \alpha^{1/4} r^{-21/8}. \quad (15)$$

This ratio is 180 times larger in a massive disc, for similar values of \dot{m} , α and r . The radius where $P_r = P_g$ is:

$$r_{\text{prg}} = 5700 m_9^{2/21} \dot{m}^{16/21} \alpha^{2/21}. \quad (16)$$

This is larger by a factor of 7 in a massive disc, compared with the light one. Thus P_r dominates over a larger part of massive discs.

2.2.2 Self-gravity

The self-gravity of the disc is $2\pi G \Sigma_0$, where $\Sigma_0 = 2\rho_0 z_0$. The ratio of self-gravity to central gravity, Q' , is:

$$Q' = 4\pi\rho_0/(M/R^3) = 1.0 \times 10^{-15} m_9 \dot{m}^{-2} r^{4.5} \alpha^{-1} \quad (17)$$

and the self-gravity radius, defined by $Q' = 1$, is:

$$r_{\text{sg}} = 2150 m_9^{-2/9} \dot{m}^{4/9} \alpha^{2/9}. \quad (18)$$

*The discussion in Section 2.2 is for the case of $P = P_r + P_g$. Similar results can be obtained for the case of $P = P_g$ and $P = \sqrt{P_g P_r}$.

Equation (18) is only approximate for $r_{\text{prg}} < r_{\text{sg}}$ since r_{sg} does not include the effects of gas pressure. Q' is proportional to m_9 , and is thus larger by a factor of $\sim 10^9$ in massive discs, for similar values of \dot{m} , α and r . The $r^{4.5}$ dependence in equation (17) results in a rapid increase of Q' beyond r_{sg} and to the probable disintegration of the disc. Whether this happens at $Q' = 1$ or 10 would only change r_{sg} by less than a factor of 2. The tendency of massive discs to become self-gravitating was discussed by Sakimoto & Coroniti (1981) and Shore & White (1982). Equation (18) suggests that r_{sg} decreases for smaller accretion rates and larger central masses. This has important consequences on the disc's spectrum, as we shall see in Section 3.

We can compare r_{sg} to r_{prg} , assuming r_{sg} is the outer edge of the disc. The ratio of these quantities depends only on L and α . For $L > 2 \times 10^{45}$ erg s $^{-1}$ and $\alpha \leq 0.1$ we get $r_{\text{prg}}/r_{\text{sg}} > 1$. This means that the high luminosity discs are radiation pressure dominated out to the radius where they become self-gravitating.

SS73 noted that the transition from $P_r > P_g$ to $P_r < P_g$ results in the disc becoming concave (i.e. $z_0 \propto r^a$ with $a > 1$). This does not occur in massive discs for $r < r_{\text{sg}}$ which we assume to be the outer boundary of the disc (see also Shore & White 1982). Thus there is no heating of the outer cool regions by the inner hot part, as suggested for example by O'Dell, Scott & Stein (1987). General relativistic bending of the paths of light rays is another effect connecting different parts of the disc. According to Cunningham (1976) and Thorne (1974) the change in the local effective temperature and in the total efficiency of the disc due to this is less than 5 per cent. Obviously the presence of some scattering material above the 'bare disc' assumed here can cause radiative connection and significant heating of some parts. This is beyond the scope of our paper.

2.2.3 Opacity

The absorption opacity, $\kappa(\text{ab})$, is proportional to $NT^{-\beta}$ ($1/2 \leq \beta \leq 3/2$), while the electron scattering opacity, $\kappa(\text{es})$, is independent of N and T . Since $NT^{-\beta} \propto m_9^{\beta/4-1}$ we find that $\kappa(\text{ab})/\kappa(\text{es})$ is smaller in massive discs. This leads to the suggestion (e.g. Callahan 1977; Begelman 1985) that Comptonization and modified blackbody spectrum, both known to be significant in stellar discs (Rees 1984, SS73), are very important in massive discs (for a description of these processes see Rybicki & Lightman 1981). Later we show that more accurate treatment of the radiative transfer shows this effect to be small in most of our models.

Next, consider the different contributions to $\kappa(\text{ab})$. For $h\nu > kT$ $\kappa_{\text{f-f}}/\kappa_{\text{b-f}} \propto T$, and since $T_{\text{eff}} \propto m_9^{-1/4}$ (assuming $T \approx T_{\text{eff}}$) the relative bound-free contribution is much larger in massive discs and can become the dominant absorption process. For example, bound-free absorption by $n=1$ of hydrogen is greater than the free-free absorption for $T < 3 \times 10^5$ K. Neglecting bound-free absorption in calculating the structure of massive discs is thus not justified. In particular, the optically thin disc, suggested by Sakimoto & Coroniti (1981) and Callahan (1977) for viscosity case (a) and f-f absorption only is avoided when the bound-free contribution is taken into account [viscosity cases (b) and (c) always result in an optically thick disc, as was demonstrated by Sakimoto & Coroniti 1981].

2.3 REQUIREMENTS FOR A THIN DISC

2.3.1 Constraints on \dot{m} and α

We define geometrically thin discs to be those where $z_0 < 0.1r$ throughout. From equation (12):

$$\frac{z_0}{r} = \frac{26.4 \dot{m} c_2}{r}, \quad (19)$$

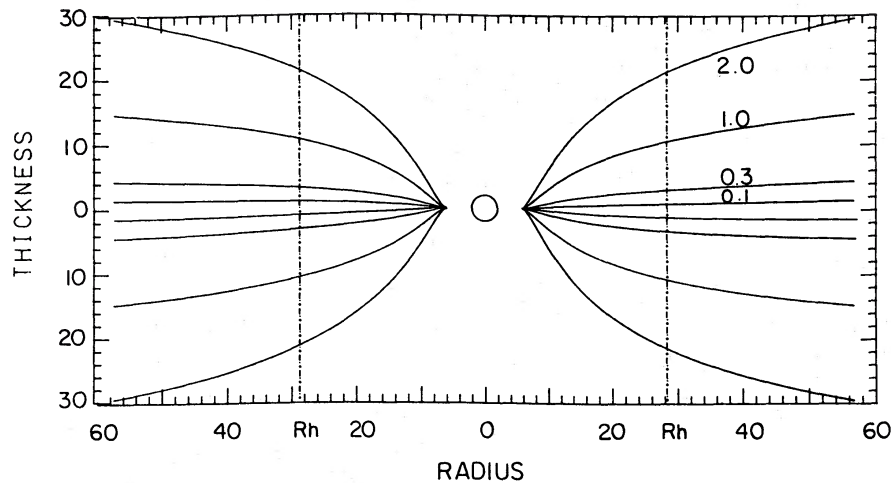


Figure 1. Disc profiles for non-rotating BH with different accretion rates. The luminosity, in units of the Eddington luminosity, is marked on the curves. The radius and the thickness are in units of R_g . R_h is the radius inside which half the total luminosity is emitted.

where c_2/r reaches a maximum of 0.015 (0.073) at $r=19$ ($r=2$) for a non-rotating (rotating) BH. The condition for a thin disc is thus $\dot{m} < 0.25$ ($L < 0.25L_{\text{edd}}$) for a non-rotating BH, and $\dot{m} < 0.033$ ($L < 0.29L_{\text{edd}}$) for a maximally rotating one. A disc radiating at the Eddington luminosity is definitely thick (see Fig. 1) and the standard disc theory, as developed by SS73 and NT73, cannot be used to calculate its spectrum. Some of the models calculated by Malkan (1983), Bechtold *et al.* (1987) and Czerny & Elvis (1987) have \dot{m} which is too large to be consistent with the thin disc model.

A similar conclusion was reached by Bisnovatyi-Kogan & Blinikov (1977) who calculated the trajectories of particles leaving the surface of the disc. For $L > 0.3L_{\text{ed}}$ these particles remain appreciably above the disc surface, and for $L > 0.5L_{\text{ed}}$ the disc is disrupted as the particles escape. The above limit on \dot{m} also guarantees that the dynamical effect of radiation pressure is unimportant. Maraschi, Reina & Treves (1976) give the critical accretion rate, $\dot{M}_c = 2R_{\text{ms}}L_{\text{edd}}/GM$, above which the radial gradient of radiation pressure results in non-Keplerian velocities. This can be translated to $\dot{m} > 2r_{\text{ms}}\eta$, which does not occur in our thin discs.

The requirement for quasi circular orbits can be translated to $V_r/V_\phi < 0.1$, where V_ϕ is the local Keplerian velocity and V_r is calculated from equation (3). This condition is:

$$\frac{V_r}{V_\phi} < 225 \frac{\dot{m}^2 \alpha c_9}{r^2}. \quad (20)$$

Using the maximum value of c_9/r^2 we find that the limit on V_r/V_ϕ implies $\dot{m}^2 \alpha < 0.36$ (0.04) for a non-rotating (rotating) BH. Note that Sakimoto & Coroniti (1981) find $V_r/V_\phi > 1$ for $r < 8$. This results from their neglect of the correction factor c_9 or its Newtonian equivalent, $1 - (r/r_{\text{ms}})^{-1/2}$.

The requirement for local energy release, combined with the assumption of radiative energy transfer, leads to another constraint on \dot{m} (see also Begelman, Blandford & Rees 1984, p. 305). The vertical radiation diffusion velocity is c/τ , where $\tau = [\kappa(\text{es}) + \kappa(\text{ab})]\Sigma_0/2$ is the optical half thickness of the disc. The condition $V_r < c/\tau$ puts a limit on the accretion rate of:

$$\dot{m} < \eta r D^{1/2}. \quad (21)$$

For this to hold down to the inner radius of the disc one needs $L < 0.28L_{\text{edd}}$ ($0.07L_{\text{edd}}$) for a non-rotating (rotating) BH. Consider for example $L = 0.3L_{\text{edd}}$ and a rotating BH. Equation (21) holds down to $r = 2$, while radiation generated at the discs midplane at $r = 1.5$ will be drifted beyond the radius of marginal stability, and probably trapped inside the BH, before reaching the surface. This results in a small correction to the spectrum from the inner part. According to Begelman (1985) there is a lower limit on m of $\sim 10^{-3}$. Below this value an ion-supported torus, rather than a disc, will be formed.

For $\alpha \approx 1$ the turbulent velocity is comparable to the sound speed, and fluctuations in the discs structure could become significant (SS73 and NT73). Canuto, Goldman & Hubickyj (1984) have shown that if the viscosity is generated by subsonic convective turbulence, than α is smaller than 0.01. In view of all the above we only consider $\alpha \leq 0.1$ and $L \leq 0.3L_{\text{edd}}$.

2.3.2 Vertical structure

The standard solution for $N(r)$ (equation 13) is obtained for $\kappa \approx \kappa(\text{es})$, instead of the more appropriate Rosseland mean opacity. We used the opacity calculation of Cox & Giuli (1968) to find the range of temperature and density for which $\kappa_{\text{ross}} \leq 2\kappa(\text{es})$. For $\log \rho < -11$ and $T > 10^4$ this is always the case. For $-11 < \log \rho < -7$ we find that the approximate relation, $\log \rho = 3.2 \log T - 23.8$, divides cases of $\kappa_{\text{ross}} < 2\kappa(\text{es})$ from cases of $\kappa_{\text{ross}} > 2\kappa(\text{es})$ in the (T, ρ) plane. Using equations (13) and (14) we can convert this to a radial dependence to find the radius, r_{es} , beyond which $\kappa_{\text{ross}} > 2\kappa(\text{es})$. We find $r_{\text{es}}/r_{\text{sg}} \approx 2.1L_{47}^{0.3}\alpha^{0.15}$, where r_{sg} is the self-gravity radius. Thus $\kappa_{\text{ross}} = \kappa(\text{es})$ is a good approximation for $r \leq 0.2r_{\text{sg}}$, and our density profile calculations, in the inner regions of the disc, are adequate. Note, however, that close to the surface of the disc the radiation field becomes significantly unisotropic and the hydrostatic equation ought to be modified to include this effect. Also, true absorption can dominate over electron scattering, due to the drop in temperature. In such a case equation (10) cannot be deduced from equation (9) and more sophisticated solutions are required.

Self-consistent calculation for the top layer has been carried out for stellar discs (e.g. Meyer & Meyer-Hofmeister 1982; Faulkner, Lin & Papaloizou 1983). Such calculations depend, critically, on the assumed viscosity mechanism, which is not known, and are not necessarily closer to reality than the rough approximations used by us.

The standard solution for the value of z_0 (the base of the photosphere) was obtained by assuming $\kappa = \kappa(\text{es})$. As seen in Fig. 2, this is not the case in some models beyond a certain radius. Equation (9) with a flux weighted mean of κ_{ν} , replacing $\kappa(\text{es})$ (see Pounds *et al.* 1987), may result in such cases in an overestimation of z_0 . More accurate atmospheric solution is required in this case. We can still get an approximate scale height for the disc by using the hydrostatic equation with a constant density:

$$P(z=0) - P(z=z_0) = \frac{GM\rho_0 z_0^2}{2R^3}. \quad (22)$$

The central pressure is (using equations 6 and 7):

$$P(z=0) = \frac{F_0 \kappa(\text{es}) z_0 \rho_0}{2c}, \quad (23)$$

and the assumption of $P(z=z_0) = 0$ gives:

$$z_0 = \frac{F_0 \kappa(\text{es}) R^3}{cGM}, \quad (24)$$

which is identical to equation (10) (relativistic corrections were neglected).

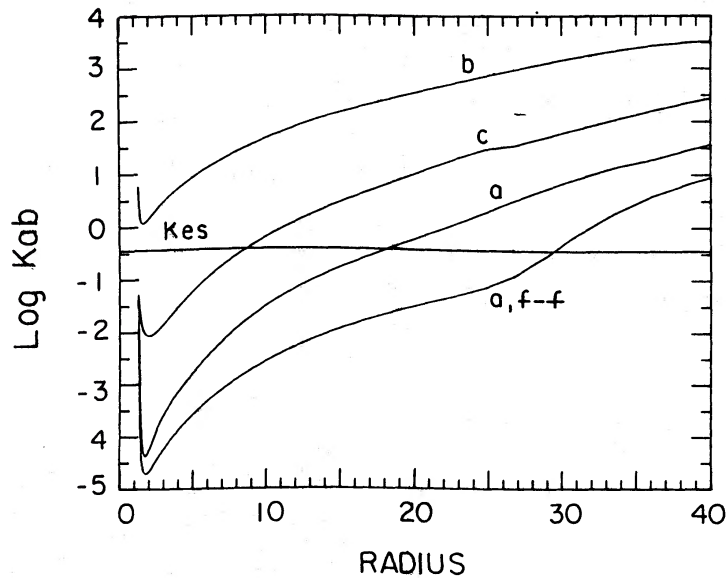


Figure 2. The flux-weighted mean absorption opacity at the disc's surface for different viscosity cases (see text) as marked on the curves. The model is of a rotating BH with $m_{\text{v}} = 0.27$, $L = 0.3L_{\text{edd}}$, and $\alpha = 0.1$. The lower curve (marked f-f) shows, for comparison, the case of free-free absorption only. The horizontal line marks the electron scattering opacity.

2.4 THE LOCAL SPECTRUM

In this section we explain our method of calculating the locally emitted spectrum. We pay special attention to electron scattering processes, and to the differences from previous calculations of this nature.

2.4.1 Opacity

We consider the following sources of opacity: free-free from hydrogen and helium, bound-free from hydrogen $n = 1$ to $n = 5$, bound-free from He^0 $n = 1, 2$, and bound-free from He^+ $n = 1, 2$. These are the main opacity sources for $T > 10^4$ K except for line opacity, which we do not consider. For $T < 10^4$ K we make a smooth transition to an arbitrary opacity of 100. The contribution of heavier elements to the opacity is neglected in order to simplify the calculations. This contribution can be significant for $\lambda < 100 \text{ \AA}$ (see Ferland & Rees 1988), but most of our models have very small flux at these wavelengths. LTE level population is assumed although this may not be strictly correct for the lowest densities considered. Our calculated flux-weighted mean of $\kappa(\text{ab})$, for the three viscosity cases, is shown in Fig. 2.

We find a significant contribution from bound-free absorption in all models, especially for $T < 10^5$ K where hydrogen and helium are not fully ionized. This was also pointed out by Czerny & Elvis (1987) but the Kramers approximation for κ_{ross} , as used by them, is inadequate since the temperature in the disc's atmosphere is too low. The commonly used assumption of free-free only (SS73, Callahan 1977; Sakimoto & Coroniti 1981; and others) is thus a poor approximation for the absorption opacity in massive discs. The opacity in viscosity cases (b) and (c) is significantly larger than in case (a) (see also Sakimoto & Coroniti 1981). Spectral modification due to electron scattering is less significant in such cases, as will be demonstrated in Section 3.

We verified that the disc is optically thick at $T < 10^4$ K, by comparison with published opacity tables (Alexander 1975). The situation described by Williams (1980) and Williams &

Ferguson (1982), where stellar discs can become optically thin, does not occur in our massive discs. Collin-Souffrin (1987) described massive discs which are optically thin in their outer region. This arises from assuming very large α (1–10), and from the neglect of self-gravity at the disc outer region.

2.4.2 Energy transfer

We use the Eddington approximation, for a grey atmosphere, to obtain the vertical temperature gradient. Using equation (6) with the boundary condition $u(\tau=0) = 2F_0/c$ and the usual assumption for stars, $q(\tau) = \text{const.}$ and $u = aT^4$, results in $T^4(\tau) = T_0^4(1 + 1.5\tau)$. The situation in discs is different since the outward flux increases from the midplane to the surface. Equation (7), with the assumption $\kappa = \kappa(\text{es})$, gives: $q(\tau) = F_0(\tau_0 - \tau)/\tau_0$, where $2\tau_0$ is the disc optical thickness, thus:

$$T^4(\tau) = T_0^4 \left(1 + 1.5\tau - \frac{3\tau^2}{4\tau_0} \right), \quad (25)$$

therefore T rises more slowly with τ compared with stars, and reaches a maximum at $\tau = \tau_0$. The temperature gradient in discs is thus smaller than in stellar atmospheres. This approximation breaks down in the outer part of the disc, where $\kappa_{\nu}(\text{abs}) > \kappa(\text{es})$ and the grey atmosphere approximation no longer holds (see below).

The Eddington approximation solution for the flux in an atmosphere in which the Planck function has a linear variation with depth [i.e. $B_{\nu}(\tau) = a_{\nu} + b_{\nu}\tau$] is given in Mihalas (1978). Below we give a more general solution for a quadratic dependence of $B_{\nu}(\tau)$. We define the absorption parameter $\lambda_{\nu} = \kappa_{\nu}(\text{ab})/[\kappa_{\nu}(\text{ab}) + \kappa(\text{es})]$ (assumed to be independent of τ), and assume $B_{\nu}(\tau) = a_{\nu} + b_{\nu}\tau + c_{\nu}\tau^2$. The Eddington approximation solution for the flux at $\tau = 0$, with the boundary condition $u(0) = \sqrt{3}F_0/c$, is:

$$F_{\nu} = \frac{4}{\sqrt{3}} \pi \left(\frac{a_{\nu}\sqrt{\lambda}}{1 + \sqrt{\lambda}} + \frac{b_{\nu}}{\sqrt{3}(1 + \sqrt{\lambda})} + \frac{2c_{\nu}}{3(\lambda + \sqrt{\lambda})} \right). \quad (26)$$

The effective optical depth is $\tau^* = \sqrt{\lambda}\tau$ and the observed photons come, on the average, from $\tau^* = 2/3$. For each frequency we calculate, using equation (25), $B_{\nu}(\tau)$ at three values of τ^* : 0, 2/3 and 4/3. The coefficients a_{ν} , b_{ν} and c_{ν} are found by fitting a second order polynomial through these points, and λ is calculated using the temperature at $\tau^* = 2/3$.

In regions where $\kappa_{\nu}(\text{ab}) > \kappa(\text{es})$ we get $\lambda \approx 1$, and the value of τ for $\tau^* = 2/3$ is independent of ν . The observed spectrum comes, on the average, from a region with the same temperature for all frequencies and F_{ν} reduces to the Planck function.

The case of an isothermal atmosphere, $b_{\nu} = c_{\nu} = 0$, has received much attention. Here:

$$F_{\nu} = \frac{4}{\sqrt{3}} \pi B_{\nu}(0) \frac{\sqrt{\lambda}}{1 + \sqrt{\lambda}}. \quad (27)$$

This case with $\sqrt{\lambda} \ll 1$ and free-free as the only source of absorption is the so-called 'modified blackbody spectrum' (e.g. Rybicki & Lightman 1981). This is considered to be important in the inner part of accretion discs (Eardly *et al.* 1978; Shapiro & Teukolsky 1983; and others). The emitted flux is reduced, in this case, considerably, compared with the Planck function, and T_0 can exceed T_{eff} by a large factor (e.g. SS73).

In our calculations T_0 is close to T_{eff} , for all cases with large optical depth, even for very small λ . This can be explained as follows: the observed photons come, on the average, from $\tau = 2/3\sqrt{\lambda}$, i.e. $\sqrt{\lambda} \ll 1$ means $\tau \gg 1$. For large vertical temperature gradient ($b_v \geq a_v$) the term $b_v \tau$ is the dominant part in $B_v(\tau)$ and the approximation $b_v = c_v = 0$ is inadequate. As a result, equation 3.7 of SS73, for the surface temperature in the region of modified blackbody emission, can result in a significant overestimation of the surface temperature. Several models calculated by Czerny & Elvis (1987) are characterized by very high temperatures. In particular, the surface temperature in some models exceeds the disc central temperature. This might be avoided if one considers the vertical temperature gradient. Note also that the vertical temperature gradient was not considered in some previous stellar discs models (e.g. Taam & Meszaros 1987).

At frequencies where $\tau^* < 1$ we make a smooth transition to the flux from an optically thin medium, with a uniform temperature of $T_c(r)$. There are difficulties for optically thin α -discs (Callahan 1977; Sakimoto & Coroniti 1981). However, the discs in our models become optically thin at such high frequencies that the flux is very small and no inconsistencies are introduced.

2.4.3 Angular flux distribution

We assume:

$$I_v(\mu_1) = I_v \frac{1}{1+a} (1 + a\mu_1), \quad (28)$$

where $a = 1.5 + 0.56(1 - \lambda)$, $\mu_1 = \cos \theta$ and θ is measured from the normal to the surface of the disc. Equation (28) reduces to the standard Eddington approximation for a grey atmosphere ($a = 1.5$) for $\kappa_{v,(\text{ab})} > \kappa(\text{es})$ and to the classical electron scattering limit ($a = 2.06$, see Sunyaev & Titarchuk 1985; Phillip & Meszaros 1986) for $\kappa(\text{es}) > \kappa_{v,(\text{ab})}$. The angular distribution is very different for $\tau_{\text{es}} < 10$ (Phillip & Meszaros 1986), but this never occurs in our model. All surface elements are assumed to be parallel to the plane of the disc. This might introduce a small error in the inner part of the largest m -discs that are seen close to edge on.

2.4.4 Comptonization

This process is important for a large value of the comptonization parameter Y where:

$$Y = \frac{4kT}{m_e c^2} \frac{\kappa(\text{es})}{\kappa(\text{ab})}, \quad (29)$$

(Rybicki & Lightman 1981). For $T = 10^5$ K, a typical temperature in massive discs, we get $Y = 10^{-4} \kappa(\text{es})/\kappa(\text{ab})$. Earlier studies (SS73; Begelman 1985) considered this process to be very important, since the local spectrum was thought to be that of a modified blackbody with maximum intensity at $\nu = 1.2kT/h$. Saturated comptonization ($Y \gg 1$), and a large shift in frequency, is expected in this case, resulting in a Wien distribution in frequencies.

We find comptonization to be of little importance because of the bound-free contribution to $\kappa(\text{ab})$, which was not considered by others. Y is very small in viscosity cases (b) and (c) where $\kappa(\text{ab})$ is large compared with $\kappa(\text{es})$ (Fig. 2). Comptonization can become significant in regions where the disc is optically thin to absorption, but this is not important in our models.

The method of calculating this process is the following: first, the local spectrum is calculated, ignoring Comptonization. All photons with $Y > 1$ are counted and redistributed in a Wien distribution, and the total flux is recalculated. The process is iterated by changing T_0 to give the required local flux. This is similar to the method described in Illarionov & Sunyaev (1972) and is accurate for $Y \gg 1$. A more accurate procedure appropriate for all Y , is described by Sunyaev & Titarchuk (1980). It requires excessive computations and depends critically on the unknown structure of the photosphere. Comptonization in a hot corona (e.g. Czerny & Elvis 1987) which is another potentially important process, was not considered in the present calculations.

2.4.5 Atmospheric calculations

An alternative approach to the local spectrum is to use stellar atmospheres with the relevant effective temperature and surface gravity, either from the literature (Kolykhalov & Sunyaev 1984; Sun & Malkan 1987) or calculated specially for this purpose (see a specific example in Pounds *et al.* 1987). Note, however, that compared with stellar atmospheres, the density in massive discs is very different (usually smaller) for the same gravity and effective temperature, and this gives a very different opacity. In addition the temperature gradient, which is largely responsible for the absorption features, is not the same in stars and discs. Complete calculations of the local spectrum require a self-consistent solution of the radiative transfer and the vertical structure of the disc, not only the atmosphere. Such calculations are bound to depend, critically, on the unknown α and viscosity law.

2.5 THE OBSERVED SPECTRUM

Adding up local contributions to obtain the observed spectrum requires a full general relativistic treatment of the propagation of radiation (Cunningham 1975, 1976). The problem is simplified for a non-rotating BH by making the following transformations, as described by Mathews (1982): The first is from the local frame of an observer rotating with the gas to that of a local observer at rest with respect to a stationary observer at infinity. The gravitational potential for both observers is the same and only special relativity is required. We then transform from the frame of the local, non-rotating observer, to that of a stationary observer at infinity. This involves gravitational redshift only (we neglected the gravitational bending of light rays). This approximation works well for a non-rotating BH, as was verified by comparing our results with those of Cunningham (1975).

The special relativistic γ factor is given in NT73. For a non-rotating BH $\gamma = \sqrt{1 - 2/r} / \sqrt{1 - 3/r}$, and we get $\gamma_{\max} = 1.15$ at $r = r_{\text{ms}} = 6$. Half the total flux of the disc is radiated, in this case, within $r \approx 30$, where $\gamma = 1.02$. The special relativistic correction to the angular distribution is given by: $\mu = (\mu' + \beta) / (1 + \beta\mu')$ (all dashed quantities refer to the disc frame, and undashed to the local non-rotating observer), where μ' is the cosine of the angle between the direction of motion of a surface element and the direction of the emitted radiation, μ is the cosine of the viewing angle, and $\beta = V_\phi/c$. This 'Doppler beaming' focuses the emitted radiation towards the plane of the disc and is especially significant in the inner, hot parts. It results in a harder spectrum at large μ . The relations for the frequency, time and solid angle transformations are: $\nu = \nu' \gamma (1 + \beta\mu') = \nu' / \gamma (1 + \beta\mu)$, $dt = dt' \gamma (1 - \beta\mu)$ and $d\Omega = d\Omega' / \gamma^2 (1 + \beta\mu')^2$. For the surface area element $ds = ds' / \gamma (1 - \beta\mu)$ where the γ factor is from the Lorentz contraction, and $(1 - \beta\mu)$ is from the fact that photons observed simultaneously from the close and far side of the area element are emitted at different times in the disc. Using the above transformations we

get:

$$I_\nu(\mu) = I'_\nu(\mu') \gamma^2 (1 + \beta \mu')^2, \quad (30)$$

which results in $F_0 = \gamma F'_0$.

Transformation to the frame of a distant observer (denoted by double dash) requires only the general relativistic redshift correction as all other factors cancel out (Mathews 1982). In this case $I''_\nu = I_\nu$ where $\nu'' = \nu \sqrt{1 - 2/r}$. The approximation is valid for a non-rotating BH, where gravitational beaming is negligible.

For a rotating BH $\gamma_{\max} = 1.22$ at $r = 1.8$ and $\gamma = 1.1$ at the half flux radius, $r = 5$. As expected the special relativistic effects are more pronounced near a rotating BH, since the disc extends to smaller radii. In this case gravitational beaming is comparable to the Doppler beaming, and the approximation used for a non-rotating BH is not valid. Instead we used the graphs and numerical process given by Cunningham (1975). This is not very accurate for angles greater than 75 degrees, where the published grid of results is not detailed enough. Note also that Cunningham's flux curves (Fig. 6) are not normalized.

To calculate the spectrum we divide the disc into 50 rings, in logarithmic steps, from the radius of marginal stability to a radius where self-gravity exceeds the central gravity. One hundred logarithmically spaced frequencies, in the range $10^{12.6} - 10^{17.4}$, are used, and the temperature at each radius is iterated to give the required local flux, integrated over this range.

For the case of a non-rotating BH we divide each ring into 80 sectors, find μ in each and transform it to the local μ' . Next we apply the limb darkening factor (equation 28) and then transform to $I_\nu(\mu)$ according to equation (30). Finally, we calculate the total flux from the sector and add contributions from all sectors. The total ring spectrum is then shifted in frequency, according to the gravitational redshift, and the process is repeated for all rings. For a rotating BH we followed instead the numerical process as described above.

3 Results

Figs 3–8 illustrate some of our results. Fig. 3(a) shows the spectra of discs with different sizes. To illustrate this case we assumed local blackbody emission for a face-on disc around a non-rotating BH. The $r_{\text{out}}/r_{\text{ms}} = 100$ disc shows practically no flat part (i.e. $F_\nu \approx \nu^0$) in its spectrum. The larger disc, with $r_{\text{out}}/r_{\text{ms}} = 1000$, produces a flat F_ν over about one octave in frequency (see also Frank, King & Raine 1985; Wade 1984) but the slope is different from the commonly assumed $\nu^{1/3}$ law. The reason for this is the correction factor $c_1 [1 - (r/r_{\text{ms}})^{-1/2}]$ in the Newtonian case, which influences the surface temperature distribution. Note that discs around white dwarfs, where the inner radius is much larger than R_g , can show a $\nu^{1/3}$ spectrum over a certain frequency range.

Fig. 3(b) compares rotating and non-rotating BH. In the first case, the disc extends much closer to the BH, and this results in a hotter atmosphere and a harder spectrum.

Fig. 3(c) illustrates the α -dependence. Smaller α means higher density and less electron scattering modification of the spectrum. The spectrum for $\alpha = 0.001$ is very close to the local blackbody approximation. The differences among different α , at the low-frequency end, are due to the fact that the larger density discs have a smaller r_{out} . A similar effect is seen in Fig. 3(d) where we show the three viscosity cases considered in this paper. The density in cases (b) and (c) is higher and the electron scattering effects smaller compared with case (a). The spectrum in case (b) is very close to the local blackbody approximation.

Fig. 4 shows spectra obtained with various approximations on the temperature structure. The constant temperature atmosphere (curve a) exhibits a large emission jump caused by the sudden increase of λ and $F_0(\nu)$ beyond the absorption edge. This is most noticeable in cases

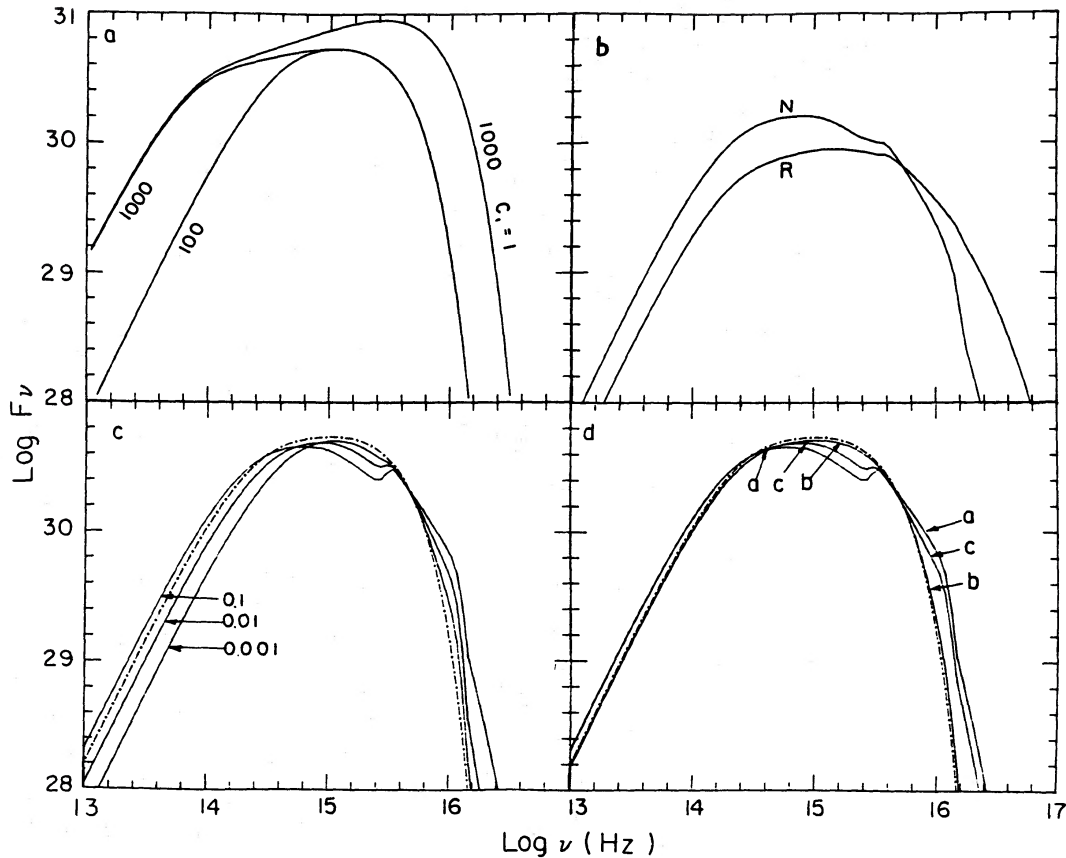


Figure 3. Spectral dependence on model parameters. Flux units here and in all following diagrams are $\text{erg s}^{-1} \text{cm}^{-2}$. All cases are for $m_g = 0.27$ and $L = 0.3L_{\text{edd}}$ ($L = 10^{46} \text{ erg s}^{-1}$). (a) A face-on non-rotating BH, with local blackbody emission and different $r_{\text{out}}/r_{\text{ms}}$ as marked. The upper curve represents the non-physical situation of $c_1 = 1$. This is the only situation where the spectrum resembles the ‘classical’ $\nu^{1/3}$ power law. (b) A comparison of rotating (R) and non-rotating (N) BH for $\theta = 60^\circ$ discs, $\alpha = 0.1$ and viscosity case (a) (the former has $r_{\text{ms}} = 1.23$ compared to $r_{\text{ms}} = 6$ for the latter). (c) α -Dependence for a face-on disc around a non-rotating BH and viscosity case (a). For comparison, the dash-dot line gives a disc with local blackbody emission. (d) Comparison of the different viscosity cases, as marked, for a face-on disc, $\alpha = 0.1$ and a non-rotating BH. The dash-dot line is the same as for (c).

where the bound-free opacity is significant. The introduction of a vertical temperature gradient (curve b) reduces this jump considerably, since the increase in λ results in a decrease in τ , thus the radiation comes from a cooler region. There is only a small difference between the cases of linear and quadratic dependence of $B(\tau)$ and we show only one of them here. Note again that the exact shape of the features depends, critically, on the nature of the transfer approximation used.

Fig. 5 shows spectra of discs with given L and different combinations of m_g and \dot{m} . The largest \dot{m} ($L = 0.3L_{\text{edd}}$) results in the hardest and flattest spectrum. Increasing m_g and decreasing \dot{m} reduces the disc temperature and the self-gravity radius. The spectrum, in this case, is narrower and softer.

Fig. 6 shows the hottest discs ($L = 0.3L_{\text{edd}}$) over a large range in luminosity. As L increases, the disc becomes cooler, due to the increase of m_g .

Fig. 7(a and b) demonstrates the angular dependence of the spectrum, caused by limb-darkening and relativistic focusing. The first of these is more significant in a non-rotating BH and the second in a rotating one, because the disc extends closer to the BH. As explained by

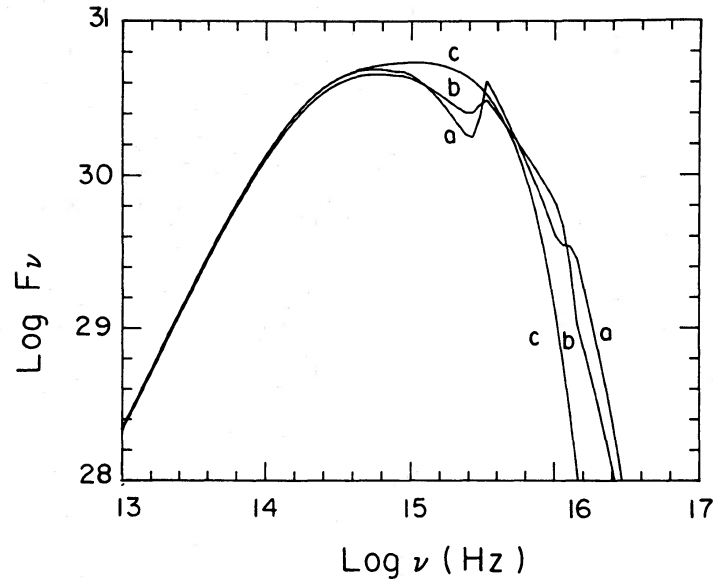


Figure 4. Flux calculations under different assumptions. Curve a: a constant temperature atmosphere. Curve b: an atmosphere with a temperature gradient. Curve c: a local blackbody approximation. All are for a face-on disc around a non-rotating BH with $\dot{m} = 0.3m_{\odot}$, $\alpha = 0.1$ and viscosity case (a).

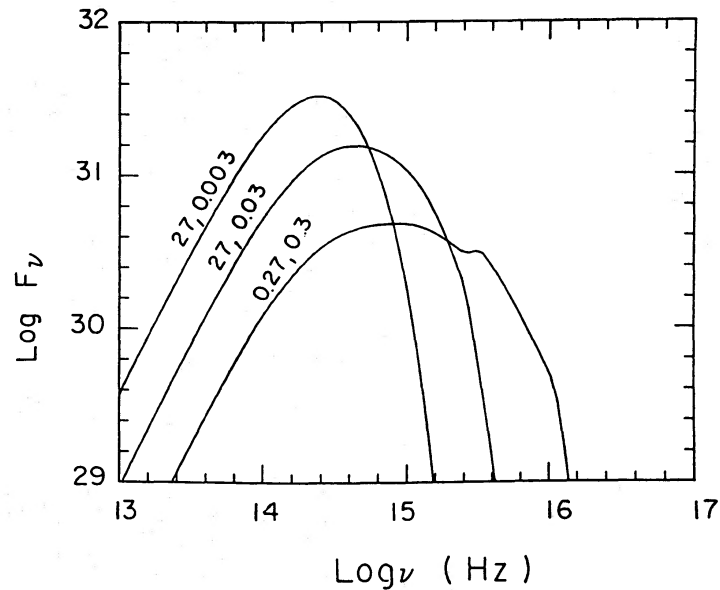


Figure 5. A face-on disc around a non-rotating BH with $L = 10^{46}$ erg s $^{-1}$. The curves show different combinations of central masses and accretion rates, marked as (m_g, \dot{m}) , resulting in the above luminosity.

Cunningham (1975), the more extreme disc becomes progressively ‘hotter’ as we move from face-on to edge-on.

Fig. 8 gives another view of the angular dependence, relevant to photoionization models of the Broad Line Region (BLR) in AGN (Netzer 1987). We show the angular dependence of the ionizing flux and the number of ionizing photons for ‘hot’ ($m_g = 0.027$, $L = 0.3L_{\text{edd}}$) and ‘cold’ ($m_g = 2.7$, $L = 0.3L_{\text{edd}}$) discs. In the ‘hot’, non-rotating BH case, Doppler focusing diverts radiation towards the plane of the disc, which reduces the effect of limb-darkening. In the ‘hot’, rotating BH case, relativistic focusing is more pronounced, and the μ -dependence almost

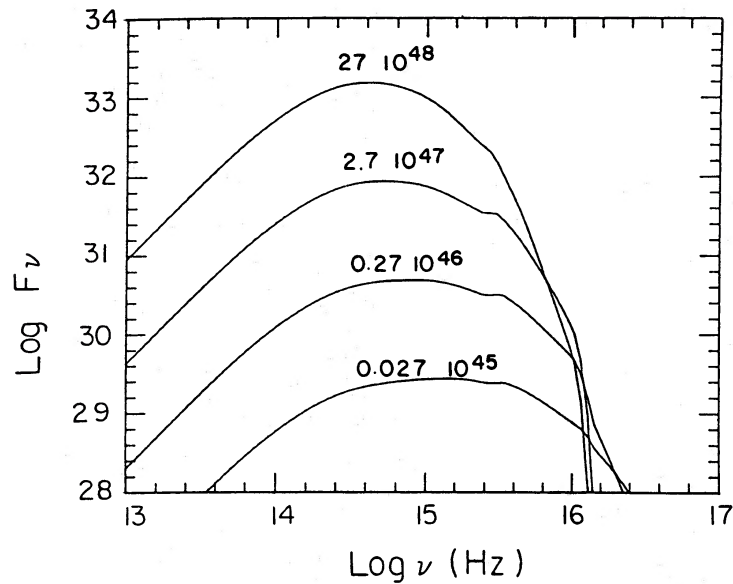


Figure 6. The hottest discs ($\dot{m}=0.3$) for different central masses and luminosities, marked as (m_g, L) . All are face-on discs around non-rotating BH.

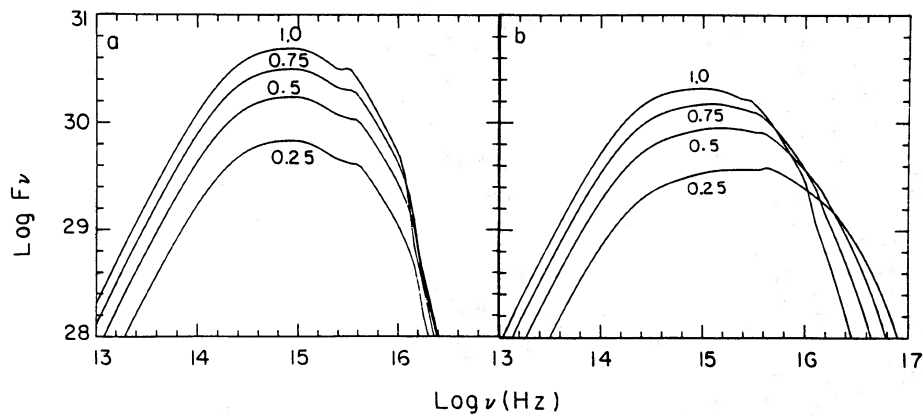


Figure 7. Viewing angle dependence (the cosine of the viewing angle is marked on the curves). $m_g=0.27$ and $L=0.3L_{\text{edd}}$, (a) a non-rotating BH, (b) a rotating BH.

disappears. Similar effects are seen in the ionizing photon flux diagram. In ‘cold’ discs relativistic effects are greater, since the ionizing radiation is emitted closer to the BH. All cases are compared with a simple μ -dependence, expected for a uniform disc with no limb-darkening.

The ionizing flux is a significant fraction of the total flux in all cases shown in Fig. 8. Some situations may be very different, for example if the Lyman limit is on the exponentially dropping part of the spectrum. In such a case a small spectral shift causes a large change in the ionizing flux.

4 Discussion

Our disc model is different from previous models in several important ways. As explained in Section 2.3, the maximum accretion rate, which is consistent with the thin disc approximation

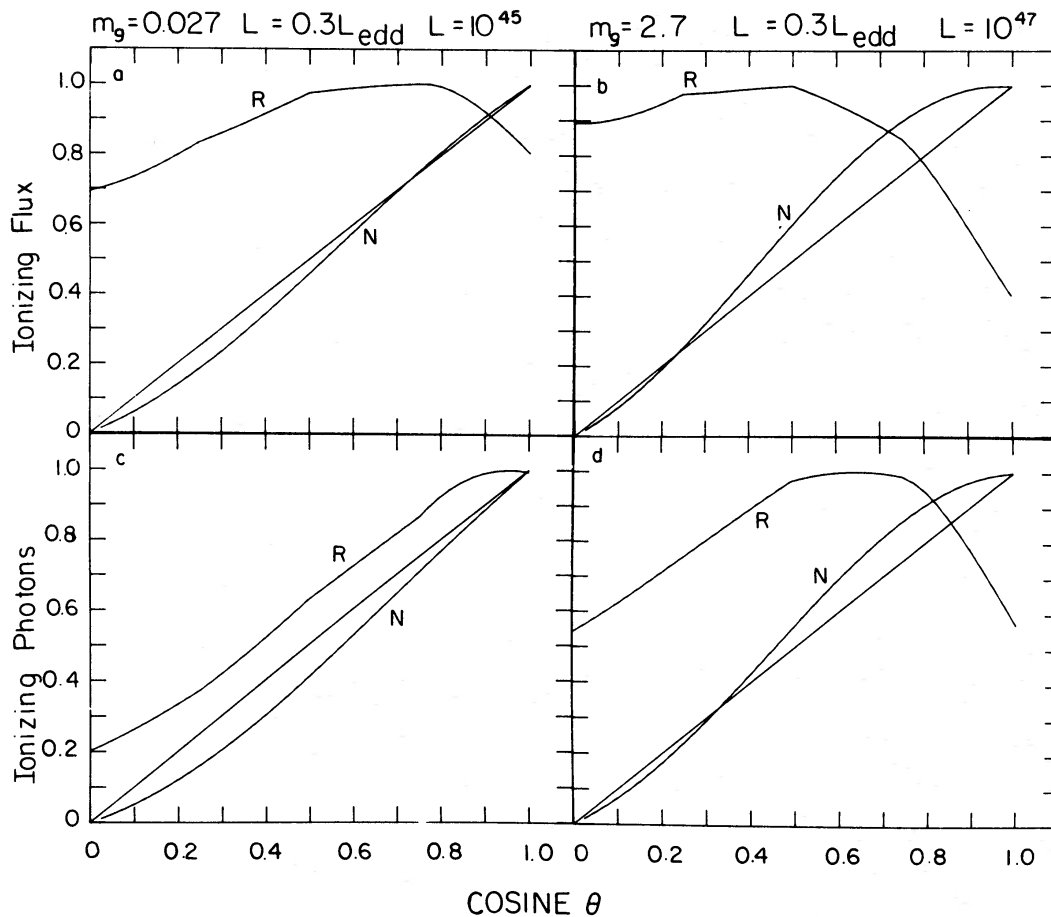


Figure 8. Ionizing radiation and photon flux at different angles. Non-rotating (rotating) BH are marked by N (R). Diagonal lines in all figures represent a simple μ dependence. (a) Flux in units of 1.2×10^{45} (9.5×10^{44}) erg s^{-1} for a non-rotating (rotating) BH. (b) Flux in units of 5×10^{46} (6.3×10^{46}) erg s^{-1} . (c) Photon flux in units of 3.2×10^{55} (1.8×10^{55}). (d) Photon flux in units of 3×10^{56} (1.6×10^{57}).

is $L \approx 0.3L_{\text{edd}}$. Some of the earlier calculations (Malkan 1983; Bechtold *et al.* 1987; Czerny & Elvis 1987) exceed this limit by a large factor and are inconsistent with the thin disc assumption. In particular, the X-ray obscuration suggested by Czerny & Elvis (1987), to explain the statistics of soft X-ray excess quasars, requires \dot{m} much larger than our limit. Our calculations take into account the vertical temperature gradient in the disc's atmosphere. This results in a surface temperature which is close to the effective temperature, while previous models (e.g. SS73; Czerny & Elvis 1987) are characterized by higher temperatures in regions where electron scattering is the dominant source of opacity. We find the effects of electron scattering to be less important compared with the model of Czerny & Elvis (1987). Such effects depend critically on the density, and are most noticeable for the viscosity case (a), large α and \dot{m} and small m_g . They are significantly less important in viscosity case (c), and practically non-existent for viscosity case (b), where the local spectrum is very close to that of a blackbody.

There have been several attempts to calculate the disc spectrum by means of stellar atmospheres with the required T_{eff} and gravity. One such model is shown in Pounds *et al.* (1987) in relation to the soft X-ray excess observed in Mrk 335. The spectrum shows strong absorption edges but no relativistic or viewing angle effects were taken into account. As already mentioned, it is not very clear how reliable such calculations are, in view of the

unknown viscosity and the intrinsically different energy production mechanism in discs compared with stars.

In Section 3 we demonstrated the dependence of the low-frequency end of the spectrum on the size of the disc. The mechanism determining the exact size of the disc is not very clear, and neither is the spectrum at those frequencies. Related to this are the calculations of the optically thin outer regions of the disc by Collin-Souffrin (1987). We suspect that the reason for the optically thin region is the high α assumed by her. Also, the value of r mentioned in that paper are, in most cases, beyond the self-gravity radius of the disc.

Our calculations show that a relatively large value of \dot{m} is needed to explain the 'big blue bump' in the spectrum of AGN. An independent constraint on \dot{m} comes from the analysis of the broad emission lines. Joly *et al.* (1985) show a possible correlation between the H_β line width and the continuum luminosity, for a large sample of AGN. Their analysis gives $L = 0.002L_{\text{edd}}$. Wandel & Yahil (1985) performed a similar study and found $L \approx 0.01L_{\text{edd}}$. Netzer (1987) re-analysed the Joly *et al.* data and concluded that $L \approx 0.03L_{\text{edd}}$ is still consistent with the observations. All these numbers are well below the value of \dot{m} required to produce the observed continuum of quasars and Seyfert galaxies by thin disc emission. The problem is most noticeable for the luminous quasars since massive discs, with such a small \dot{m} and large m_9 , produce a narrow and soft continuum, which is inconsistent with the observations. The disagreement between the required and 'observed' \dot{m} is an obvious problem for further study.

Assuming AGN to be powered by thin accretion discs, with a small range of \dot{m} , we expect the frequency of maximum emission to be lower for larger M and L . Preliminary work by Wandel (1987) indicates that this is perhaps observed. Unfortunately, his simplified $\nu^{1/3}$ disc spectrum, with no angular dependence, is a very rough approximation to the disc spectrum. We are currently looking into this, using our improved models.

We find the most luminous discs, those with $L > 10^{46}$ erg s $^{-1}$, to be too cold to emit significantly at $\lambda < 100$ Å (Fig. 6). It might thus be impossible to explain the soft X-ray excess in quasars as due to thermal thin disc emission. Comptonization in a hot corona, can produce a significant X-ray flux (e.g. Czerny & Elvis 1987) but we did not attempt to calculate it here.

The angular distribution of the ionizing flux has important consequences for the broad line spectrum (Netzer 1987). As shown in Section 3, the distribution can be very different for different discs. The limb darkening law used by Netzer (1987) gives a good approximation in some cases [Fig. 8(a) non-rotating BH] and a poor one in others [Fig. 8(b) rotating BH]. Further modelling of the broad line spectrum, in the presence of a central disc, is a potential source of information that ought to be investigated further.

Several general comments about thermal emission in AGN are in order. Short time-scale X-ray variability of AGN suggests the existence of a central small ionizing source (e.g. Barr & Mushotzky 1986). The X-ray source may be separated from the disc component. It can photoionize the disc's photosphere and modify the emitted spectrum (Shields 1978). This is only one out of several possible configurations suggested to explain AGN ultraviolet emission. Thin 'bare' discs may well be a simplified, zero-order, approximation for a more complicated situation.

An alternative approach to thermal emission in AGN was taken by Ferland & Rees (1988) who calculated the spectrum of small gas clouds immersed in an intense non-thermal radiation field. Their model produces a blue bump not too different from those calculated in some disc models.

Finally, a general warning about the α disc model. Case (a) of the α disc [$t_{r\phi} = \alpha(P_r + P_g)$], is known to be thermally and secularly unstable in the radiation pressure dominated region (Piran 1978). It is not known whether this results in a time-dependent structural change, or a

complete destruction of the disc. Cases (b) ($t_{r\phi} = \alpha P_g$) and (c) ($t_{r\phi} = \alpha \sqrt{P_r P_g}$) are probably stable. A more serious limitation is the assumption of a constant α , which is an extreme simplification. There have been some attempts to improve the α prescription (Meyer & Meyer-Hofmeister 1982; Canuto, Goldman & Hubickyj 1984, and others) but the main viscosity mechanism is still unknown.

Acknowledgments

We thank I. Shlosman and I. Goldman for useful information and discussions, and the Binational Science Foundation for financial support through grant no. 85/00085.

References

- Alexander, D. R., 1975. *Astrophys. J. Suppl.*, **29**, 363.
 Barr, P. & Mushotzky, R. F., 1986. *Nature*, **320**, 421.
 Bechtold, J., Czerny, B., Elvis, M., Fabbiano, G. & Green, R. F., 1987. *Astrophys. J.*, **314**, 699.
 Begelman, M. C., 1985. In: *Astrophysics of Active Galaxies and Quasi-Stellar Objects*, p. 411, ed. Miller, J. S., University Science Books, Mill Valley, CA.
 Begelman, M. C., Blandford, R. D. & Rees, M. J., 1984. *Rev. mod. Phys.*, **56**, 225.
 Bisnovatyi-Kogan, G. S. & Blinikov, S. P., 1977. *Astr. Astrophys.*, **59**, 111.
 Burm, H., 1985. *Astr. Astrophys.*, **143**, 389.
 Callahan, P. S., 1977. *Astr. Astrophys.*, **59**, 127.
 Cannizo, J. K. & Wheeler, J. C., 1984. *Astrophys. J. Suppl.*, **55**, 367.
 Canuto, V. M., Goldman, I. & Hubickyj, D., 1984. *Astrophys. J.*, **280**, L55.
 Collin-Souffrin, S., 1987. *Astr. Astrophys.*, **179**, 60.
 Cox, J. P. & Giuli, R. T., 1968. *Principles of Stellar Structure*, Vol. I, p. 397, Gordon & Breach, New York.
 Cunningham, C. T., 1975. *Astrophys. J.*, **202**, 788.
 Cunningham, C. T., 1976. *Astrophys. J.*, **208**, 534.
 Czerny, B. & Elvis, M., 1987. *Astrophys. J.*, **312**, 325.
 Eardly, D. M., Lightman, A. P., Payne, D. G. & Shapiro, S. L., 1978. *Astrophys. J.* **224**, 53.
 Faulkner, J., Lin, D. N. C. & Papaloizou, J., 1983. *Mon. Not. R. astr. Soc.*, **205**, 359.
 Ferland, G. J. & Rees, M. J., 1988. *Astrophys. J.*, **332**, 141.
 Frank, J., King, A. R. & Raine, D. J., 1985. *Accretion Power in Astrophysics*, p. 85, Cambridge University Press, Cambridge.
 Herter, T., Lacasse, M. G., Wesemael, F. & Winget, D. E., 1979. *Astrophys. J. Suppl.*, **39**, 513.
 Kolykhalov, P. L. & Sunyaev, R. A., 1984. *Adv. Space Res.*, **3**, 249.
 Kriz, S. & Hybeny, I., 1987. *Astrophys. Space Sci.*, **130**, 341.
 Illarionov, A. F. & Sunyaev, R. A., 1972. *Soviet Ast.*, **16**, 45.
 Joly, M., Collin-Souffrin, S., Masnou, J. L. & Nattale, L., 1985. *Astr. Astrophys.*, **152**, 282.
 Lin, D. C. & Shields, G. A., 1986. *Astrophys. J.*, **305**, 28.
 Malkan, M. A., 1983. *Astrophys. J.*, **268**, 582.
 Malkan, M. A. & Sargent, W. L., 1982. *Astrophys. J.*, **254**, 22.
 Maraschi, L., Reina, C. & Treves, A., 1976. *Astrophys. J.*, **206**, 295.
 Mathews, W. G., 1982. *Astrophys. J.*, **258**, 425.
 Meyer, F. & Meyer-Hofmeister, E., 1982. *Astr. Astrophys.*, **106**, 34.
 Mihalas, D., 1978. *Stellar Atmospheres*, 2nd edn, p. 148, eds Burbidge, G. & Burbidge, M., Freeman, San Francisco.
 Netzer, H., 1987. *Mon. Not. R. astr. Soc.*, **225**, 55.
 Novikov, I. & Thorne, K. S., 1973. In: *Black Holes*, p. 422, eds de Witt, C. & de Witt, B., Gordon & Breach, New York (NT73).
 O'Dell, S. L., Scott, H. A. & Stein, W. A., 1987. *Astrophys. J.*, **313**, 164.
 Page, D. N. & Thorne, K. S., 1974. *Astrophys. J.*, **191**, 499 (PT74).
 Pounds, K. A., Stanger, V. J., Turner, T. J., King, A. R. & Czerny, B., 1987. *Mon. Not. R. astr. Soc.*, **224**, 443.
 Phillip, K. C. & Meszaros, P., 1986. *Astrophys. J.*, **310**, 284.
 Piran, T., 1978. *Astrophys. J.*, **221**, 652.
 Pringle, J. E., 1981. *Ann. Rev. Astr. Astrophys.*, **19**, 137.

- Rees, M. J., 1984. *Ann. Rev. Astr. Astrophys.*, **22**, 471.
- Rybicki, G. B. & Lightman, A. P., 1981. *Radiative Processes in Astrophysics*, Wiley, New York.
- Sakimoto, P. J. & Coroniti, F. V., 1981. *Astrophys. J.*, **247**, 19.
- Shakura, N. I. & Sunyaev, R. A., 1973. *Astr. Astrophys.*, **24**, 337 (SS73).
- Shakura, N. I. & Sunyaev, R. A., 1976. *Mon. Not. R. astr. Soc.*, **175**, 613 (SS76).
- Shakura, N. I., Sunyaev, R. A. & Zilitinkevich, S. S., 1978. *Astr. Astrophys.*, **62**, 179.
- Shapiro, S. L. & Teukolsky, S. A., 1983. *Black Holes, White Dwarfs, and Neutron stars*, Wiley, New York.
- Shields, G., 1978. *Nature*, **272**, 706.
- Shore, S. N. & White, R. L., 1982. *Astrophys. J.*, **256**, 390.
- Sun, W. H. & Malkan, M. A., 1987. In: *Astrophysical Jets and Their Engines*, ed. W. Kundt, Reidel, Dordrecht.
- Sunyaev, R. A. & Titarchuck, L. G., 1980. *Astr. Astrophys.*, **86**, 121.
- Sunyaev, R. A. & Titarchuck, L. G., 1985. *Astr. Astrophys.*, **143**, 374.
- Taam, R. E. & Meszaros, P., 1987. *Astrophys. J.*, **322**, 329.
- Thorne, K. S., 1974. *Astrophys. J.*, **191**, 507.
- Wade, R. A., 1984. *Mon. Not. R. astr. Soc.*, **208**, 381.
- Wandel, A., 1987. *Astrophys. J.*, **316**, L55.
- Wandel, A. & Yahil, A., 1985. *Astrophys. J.*, **295**, L1.
- Williams, G. A., King, A. R. & Brooker, J. R. E., 1987. *Mon. Not. R. astr. Soc.*, **266**, 725.
- Williams, R. E., 1980. *Astrophys. J.*, **235**, 939.
- Williams, R. E. & Ferguson, D. H., 1982. *Astrophys. J.*, **257**, 672.